Proc. Natl. Acad. Sci. USA
Vol. 75, No. 8, pp. 3742–3746, August 1978
Biochemistry

High-resolution ^{13}C nuclear magnetic resonance studies of glucose metabolism in *Escherichia coli*

(glycolysis/glucose utilization/anomeric specificity/anaerobic/aerobic)

K. UGURBIL, T. R. BROWN, J. A. DEN HOLLANDER, P. GLYNN, AND R. G. SHULMAN

Bell Laboratories, 600 Mountain Ave., Murray Hill, New Jersey 07974

Contributed by R. G. Shulman, June 9, 1978

ABSTRACT **High-resolution ^{13}C nuclear magnetic resonance spectra of suspensions of *Escherichia coli* cells have been obtained at 90.5 MHz by using the Fourier transform mode. Anaerobic cells incubated with [*1*-^{13}C]glucose show a time course of glycolysis in which the α and β glucose anomers disappear at different rates, lactate, succinate, acetate, alanine, and valine accumulate as end products of glycolysis, and fructose bisphosphate appears as an intermediate. It is shown that fructose bisphosphate is labeled at C-1 and C-6 during [*1*-^{13}C]-glucose catabolism. Upon oxygenation, glutamate appears with the ^{13}C enrichment at the C-4, C-3, and C-2 positions, with the C-4 most intense. From the position of the ^{13}C label we conclude that valine is formed by condensation of pyruvate and that carbon enters the tricarboxylic acid cycle mainly through acetyl CoA.**

^{31}P high-resolution nuclear magnetic resonance (NMR) studies of cellular suspensions and of intact tissue have shown how this noninvasive technique can follow concentrations and kinetics of metabolites *in vivo* (1–3). Because several phosphate metabolites have chemical shifts that are sensitive to pH under physiological conditions, it has also been possible to distinguish intracellular and extracellular pH values (2–5). Although ^{31}P NMR has been valuable in studying cellular problems, it is restricted to monitoring phosphorylated metabolites.

In the present report we show that it is possible to observe well-resolved ^{13}C NMR of numerous metabolites in anaerobic and aerobic suspensions of *Escherichia coli* cells and to assign certain resonances to particular carbons of transient intermediates as well as of end products. End-product enrichment by the use of labeled ^{13}C compounds has been reported. When ^{13}C-enriched glucose was fed to yeast, two weak, barely resolved resonances from end products of glycolysis were detected by ^{13}C NMR (6). More recently, ^{13}C spectra of intact soybean ovules (7) and erythrocytes (8) exposed to $^{13}CO_2$ have been reported and some long-lived compounds have been identified.

Biosynthetic pathways have been followed by feeding various ^{13}C-labeled substrates to different microorganisms and measuring the ^{13}C NMR spectra of extracts (9–12). ^{13}C NMR spectra of labeled macromolecules have been obtained in whole cells before extraction (13, 14). Recently, glucose utilization was measured by natural-abundance ^{13}C NMR in suspensions of acetone-treated yeast cells in which the cell membranes were rendered permeable and the rate of glycolysis was decreased ~100-fold, thus allowing long accumulation times (15).

In the present study we used ^{13}C-enriched glucose and a high-frequency ^{13}C NMR spectrometer to monitor metabolism in anaerobic and aerobic *Escherichia coli* suspensions. We followed the time course of glucose metabolism in well-resolved spectra obtained with 1-min accumulations and identified intermediates as well as end products. Furthermore, we observed that more than one position on several intermediates were labeled with ^{13}C during catabolism of glucose enriched only at C-1. The distribution of the ^{13}C label among the different carbons of these intermediates and of the end products allows one to follow pathways in considerable detail *in vivo* and to evaluate the relative rates of alternate reactions that lead to "scrambling" of the label. It is important to note that these NMR experiments uniquely determined *in vivo* the extent of labeling among intermediates that may have rapid turnover rates, and thus they avoid the uncertainties encountered in extracting such metabolites.

EXPERIMENTAL SECTION

E. coli strain MRE 600 were grown aerobically at 37° in M9 minimal medium supplemented with 20 mM glucose and 0.1 mM $CaCl_2$. Cells were harvested at midlogarithmic phase and collected by centrifugation at 4°C as described (3). Recovered pellets were washed twice and resuspended in an equal volume of cold buffered medium (specified in figure legends) that lacked nitrogen and carbon sources.

^{13}C NMR spectra were obtained at 90.52 MHz on a Bruker HX-360 spectrometer equipped with a 10-mm ^{13}C probe and operating in the Fourier transform mode. A repetition time of 0.34 sec and 60° pulses were used.

[*1*-^{13}C]Glucose was purchased from Merck and used to prepare [*1,6*-^{13}C]fructose bisphosphate (Fru-1,6-P_2) enzymatically.

All chemical shifts were referred to tetramethylsilane through the use of the α C-1 glucose resonance at 92.97 ppm as an internal reference. The high density of cells used in our cell suspensions automatically rendered the NMR samples anaerobic. For aerobic experiments, cells were oxygenated by bubbling O_2 through the samples at the rate of 18 ml/min.

RESULTS

Fig. 1 shows a sequence of ^{13}C NMR spectra of a suspension of anaerobic *E. coli* cells measured at different times after glucose addition. The resonances have been assigned on the basis of chemical shift information (16–18) and considerations of the known metabolic pathways. The Fru-1,6-P_2 assignment has been checked in cell extracts as discussed below. Prior to glucose addition, only the natural abundance ^{13}C resonances of the buffers (labeled B) used in the external medium were detectable. After addition of [*1*-^{13}C]glucose there appeared at 0.5 min the well-resolved α and β peaks of [*1*-^{13}C]glucose as well as several weak resonances that stem from the natural abundance

The costs of publication of this article were defrayed in part by the payment of page charges. This article must therefore be hereby marked "*advertisement*" in accordance with 18 U. S. C. §1734 solely to indicate this fact.

Abbreviations: NMR, nuclear magnetic resonance; Fru-1,6-P_2, fructose bisphosphate; Mes, 2-(*N*-morpholino)ethanesulfonic acid; Pipes, 1,4-piperazinediethanesulfonic acid; Glc-6-*P*, glucose 6-phosphate.

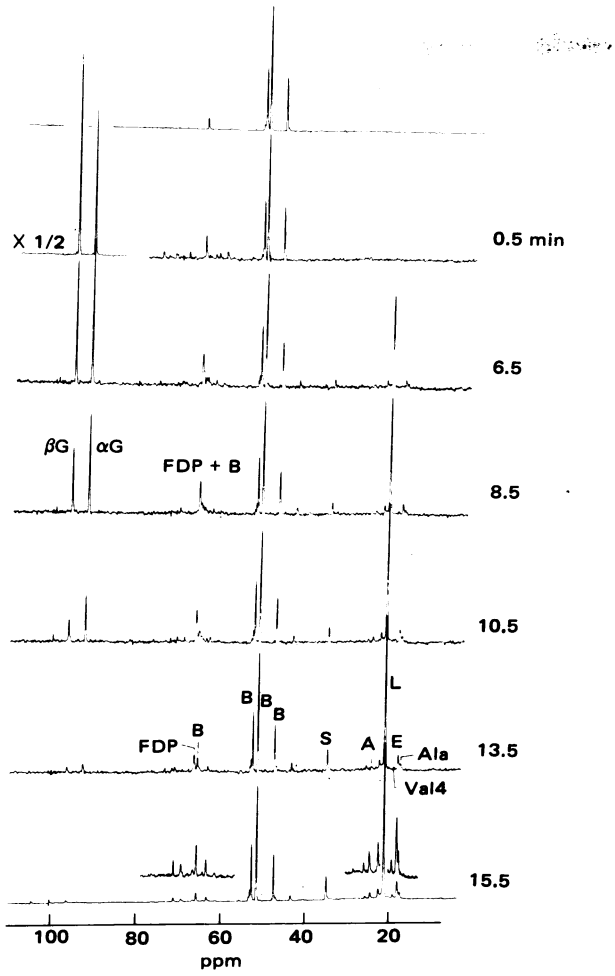

FIG. 1. The 90.52-MHz ^{13}C NMR spectra of anaerobic *E. coli* cells at 20°C as a function of time from ^{13}C-1 glucose addition. The cells were suspended in 10 mM Na_2HPO_4 10 mM KH_2PO_4 200 mM 1,4-piperazinediethanesulfonic acid (Pipes)/50 mM 2-(*N*-morpholino)ethanesulfonic acid (Mes), pH 7.5 (adjusted with NaOH), at a density of ~5 × 10^{11} cells per ml. [1-^{13}C]Glucose was added to a final concentration of 50 mM in the NMR sample, at time 0. Top spectrum (1600 scans) shows the natural-abundance ^{13}C peaks (assigned to the Pipes and Mes buffers) detectable in the suspension prior to glucose addition. All subsequent spectra, except the last one, represent 200 free induction decays accumulated in 1 min. The last spectrum consists of 1600 scans. The time given for each spectrum indicates the middle of the accumulation period, referred to glucose addition. FDP, Fru-1,6-P_2; see text for other abbreviations.

^{13}C nuclei at the other positions of the two glucose anomers. At 2 min, a strong lactate peak (L) and a weaker succinate peak (S) appeared and the intensities of the glucose peaks decreased, the β glucose preferentially. Initially, the chemical shift of the C-1 β-Fru-1,6-P_2 resonance coincided with that of the smallest buffer peak (at 66.7 ppm). At later times, as seen in the 13.5-min spectrum, this small buffer peak moved slightly to higher fields due to acidification of the extracellular medium during glycolysis; consequently, it is resolved from the C-1 β-Fru-1,6-P_2 peak. The other resonances detectable in the 13.5 min spectrum have been assigned to the methyl groups of acetate (A), ethanol (E), alanine (Ala), and valine (Val4) (18). At 15.5 min the Fru-1,6-P_2 peak disappeared and only those resonances that stem from the end products of glucose catabolism remained detectable. Five of these resonances, located at 71.1, 69.4, 43.7, 25.3, and 22.2 ppm, have not yet been identified. As long as the cells were kept anaerobic, no further developments in the end product resonances were observed for several hours.

Upon oxygenation of the sample, the ^{13}C NMR spectrum evolved in time (Fig. 2). Each of these spectra represents ~8 min of accumulation. The intensities of the resonances that were observed at the end of the anaerobic run changed with time in the presence of O_2. Additional resonances also become detectable. Six of these new peaks have been assigned, on the basis of their chemical shifts, to C-2, C-3, and C-4 of glutamate (Glu) and glutamine (Gln). Four new resonances with chemical shifts 58.3, 49.9, 45.7, and 23.1 ppm remain unidentified. Except for the 45.7 peak, these unidentified peaks were very small.

The intensities of the major resonances shown in Figs. 1 and 2 are plotted as a function of time in Figs. 3 and 4 for the anaerobic and the aerobic runs, respectively (the data for Fig. 4 were obtained from the experiments shown in Fig. 2; Fig. 3 was prepared from an experiment done under conditions identical to those of Fig. 1 except the Mes buffer in the suspension medium was replaced with Pipes in order to avoid interference with the C-1 β-Fru-1,6-P_2 resonance). At ~1.5 min after glucose addition, a constant Fru-1,6-P_2 concentration was reached and maintained for ~6 min (Fig. 3). When the total glucose level decreased to ~7% of its initial intensity (at 8.5 min), a decrease in Fru-1,6-P_2 intensity and lactate production occurred. At ~11.5 min, glucose (and at 13.5 min, Fru-1,6-P_2) could no longer be detected. Oxygenation led to a rather rapid decrease in the lactate intensity. Succinate and acetate initially built up and then decreased after lactate had been consumed.

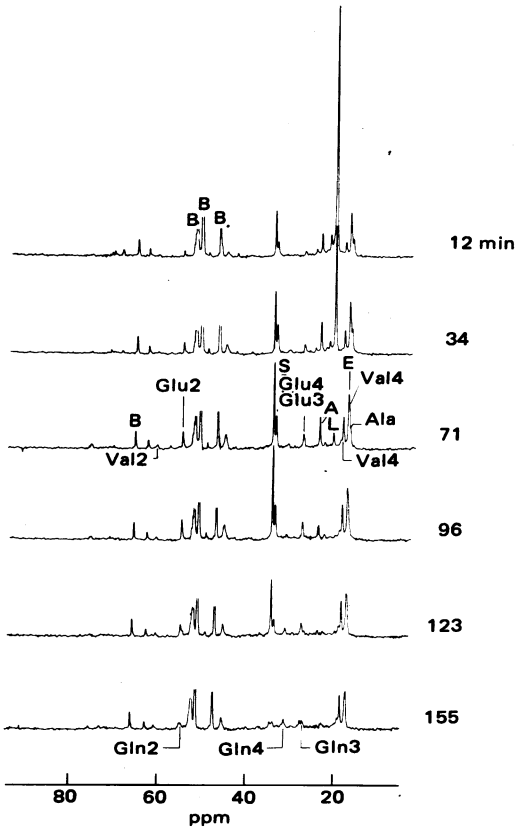

FIG. 2. The 90.52-MHz ^{13}C NMR spectra of aerobic *E. coli* cells at 20°C as a function of time from oxygenation. The sample is the same as in Fig. 1. At 3 min after the bottom spectrum in Fig. 1 was obtained, cells were oxygenated by bubbling O_2 through them at the rate of 18 ml/min. Each spectrum represents an average of 1600 free induction decays obtained in ~8 min. Times given indicate the middle of the accumulation period from the start of oxygenation. See text for abbreviations.

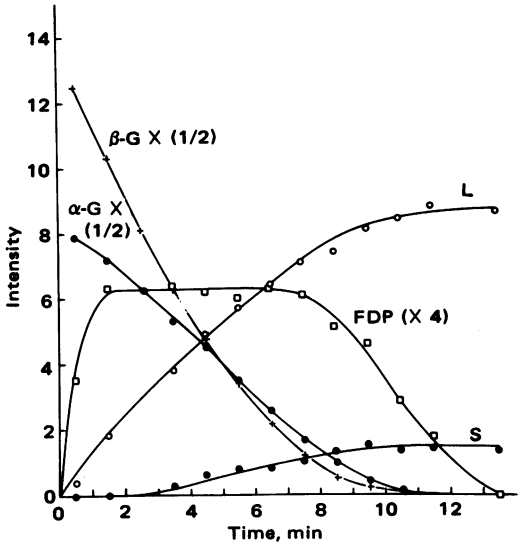

FIG. 3. Peak intensities of the major detectable ^{13}C resonances in anaerobic *E. coli* cells as a function of time from [1-^{13}C]glucose addition. Peak intensities (heights) are given in arbitrary units. Data were obtained from an experiment performed under conditions identical to those of Fig. 1 except the resuspension medium contained 250 mM Pipes instead of 200 mM Pipes and 50 mM Mes. FDP, Fru-1,6-P_2.

DISCUSSION

It is clear from these results that the ^{13}C-enriched metabolites give *in vivo* spectra that are better resolved than corresponding ^{31}P NMR spectra and have slightly better signal-to-noise ratios even though the smaller nuclear moment reduces the ^{13}C intensity to approximately one-fourth. The resolution is better because the ^{13}C full-widths at half-height are ~15 Hz at 90.5 MHz (except for the β-Fru-1,6-P_2 peak whose width is ~30 Hz); at the same magnetic field and 145.7 MHz, the ^{31}P widths range from 35 to 90 Hz. Furthermore, the range of ^{13}C chemical shifts in the abundant metabolites is ~100 ppm as opposed to ~20 ppm for ^{31}P in the corresponding phosphates. The ^{13}C sensitivity is improved 2- or 3-fold with respect to ^{31}P by the narrower lines. Presumably, the nuclear Overhauser effect is contributing another factor of almost 3 which would explain the observed intensities, but this must still be tested.

E. coli is a "mixed-acid" bacterium and is expected to produce lactate, acetate, succinate, and formate as well as ethanol and glycerol during anaerobic glycolysis (19). Formate will not contain a label when [1-^{13}C]- or [6-^{13}C]glucose is used as the carbon source; therefore, it will not be detectable in our spectra. Glycolysis in strain MRE 600 under our conditions (see Figs. 1 and 3) produces mainly lactate which presumably is derived directly from pyruvate by the action of lactate dehydrogenase. Succinate, ethanol, and acetate are produced to a much lesser extent. The relative distributions of these four metabolites under our conditions is somewhat different from previously reported values (19). However, the ratios of the end products formed may depend on environmental conditions and may even vary among different strains.

The two amino acids, valine and alanine, that are synthesized during anaerobic catabolism of glucose belong to the "pyruvate" class of amino acids. Alanine is thought to be synthesized by amination of pyruvate using glutamate as the amino group donor (20). Each molecule of valine on the other hand is expected to be produced from two pyruvate molecules by a mechanism that should label exclusively the two methyl (C-4) carbons (20). One of the two methyl carbon resonances appears at 18.9 ppm (labeled Val4 in Fig. 1). The second is discernible as a shoulder on the ethanol peak but is not well resolved.

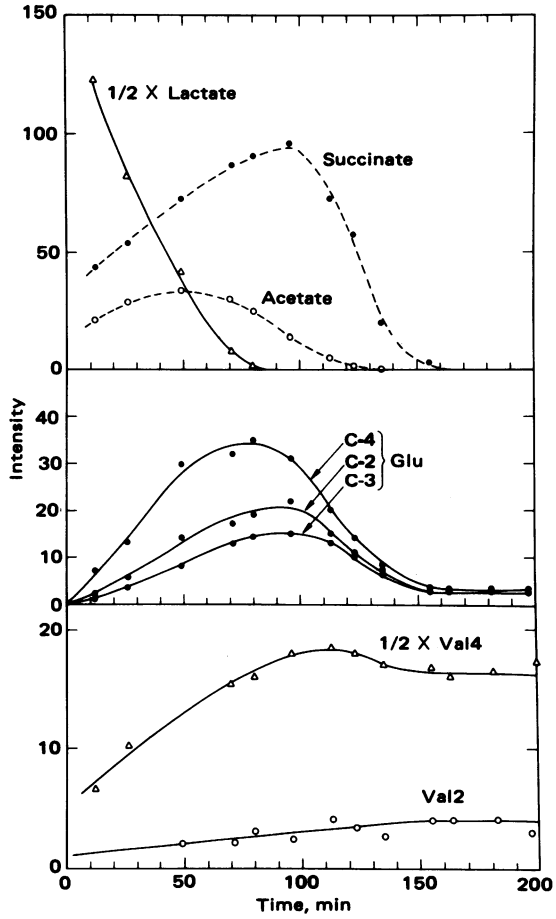

FIG. 4. Peak intensities of major resonances in aerobic *E. coli* cells as a function of time from the onset of oxygenation. Data were obtained from the experiment shown in Fig. 2.

However, when cells are oxygenated, overall valine intensity increases and this second methyl carbon (also labeled Val4) becomes more prominent (see Fig. 2). The weak intensity of Val2 relative to Val4 shown in Fig. 2 indicates that the pyruvate pathway dominates the biosynthesis of valine even during aerobic conditions.

During anaerobic glycolysis, Fru-1,6-P_2 is the only intermediate of the Embden–Meyerhof–Parnas pathway that is present in large quantities. This was anticipated from the results of analogous ^{31}P NMR experiments performed under similar conditions (3). From the ^{31}P NMR experiments (3), the intracellular concentration of Fru-1,6-P_2 at its maximum was estimated to be ~13 mM. The only other intermediate of this pathway that we have positively identified is glucose 6-phosphate (Glc-6-*P*) which was observed in the *in vivo* ^{13}C NMR spectrum when [6-^{13}C]glucose was used as the glycolysis substrate. The chemical shift of C-1 of Glc-6-*P* is very similar to that of the C-1 of glucose and is not resolved from the intense glucose C-1 resonances in the intact cell spectrum. From a spectrum obtained by using [6-^{13}C]glucose, we estimate the intracellular Glc-6-*P* concentration to be ~2 mM. Glc-6-*P* and dihydroxyacetone phosphate were also identified in the previously reported ^{31}P NMR spectra of *E. coli* cell extracts, prepared under similar conditions (3). In *E. coli*, as much as 25% of the glucose may be catabolized via the pentose shunt (19). When [1-^{13}C]glucose is the carbon source, the label will be lost as CO_2 in the phosphogluconate dehydrogenase step of the pentose shunt.

The Fru-1,6-P_2 region of the ^{13}C NMR spectra of glycolysing *E. coli* cells is illustrated with a better signal-to-noise ratio in

Fig. 5. Peaks 1 and 2, located at 71.1 and 69.4 ppm, are from the two unidentified end products of glycolysis that have already been mentioned. Peak 3 had a time dependence similar to that of Fru-1,6-P_2 and also remains unidentified. Peak 4 stems from an impurity in the [1-^{13}C]glucose used. The peaks labeled βFDP-C1, αFDP-C1 and βFDP-C6 are at 66.6, 65.8, and 65.3 ppm, respectively. The relative intensities of the β and α resonances indicate that the Fru-1,6-P_2 anomers are approximately in equilibrium (21).

Note that the resonance located at 65.3 ppm has been assigned to C-6 carbon of β-Fru-1,6-P_2. In view of the importance of this assignment in isotopic exchange considerations, we have tested it by two methods. Fig. 6*b* shows the Fru-1,6-P_2 region of the ^{13}C NMR spectrum of an *E. coli* cell extract obtained 5 min after glucose addition. This sample was then divided into two portions. To one we added a small amount of Fru-1,6-P_2 prepared enzymatically from [1-^{13}C]glucose so as to contain approximately equal fractions of ^{13}C at the 1 and 6 carbons. The resulting spectrum is shown in Fig. 6*a*. The newly added Fru-1,6-P_2 appeared directly on top of the resonances assigned to C-1 and C-6 of Fru-1,6-P_2, with no sign of any splitting, strongly supporting the assignments. The other half of the original extract sample was incubated with a small amount of hexosediphosphatase for several hours, and subsequently it gave the spectrum shown in Fig. 6*c*. The resonance assigned to C-1 of α- and β-Fru-1,6-P_2 in Fig. 6*b* almost completely disappeared in Fig. 6*c* and a new peak at 63.6 ppm appeared exactly where C-1 of Fru-6-*P* is expected. Furthermore, the peak assigned to C-6 of Fru-1,6-P_2 in Fig. 6*b* was replaced by a resonance that was broader and shifted slightly downfield, as expected for the conversion of Fru-1,6-P_2 C-6 to Fru-6-*P*.

In order to test the assignments further, especially that of Fru-1,6-P_2 C-6, a small amount of phosphohexose isomerase was added to the sample after the spectrum shown in Fig. 6*c* was obtained. The resulting spectrum is illustrated in Fig. 6*d*. The resonance assigned to C-6 of Fru-6-*P* virtually disappeared and the intensity of the Fru-6-*P* C-1 peak was substantially reduced. This is expected because the isomerase catalyzes the conversion of Fru-6-*P* to Glc-6-*P* and the latter is 3 times more concentrated at equilibrium. The C-6 resonance of Glc-6-*P* coincides, within our resolution, with that of Fru-6-*P* C-1; consequently, the Fru-6-*P* C-1 resonance of Fig. 6*c* is replaced with the combined peak. We could not independently test for the appearance of Glc-6-*P* in the spectra after addition of

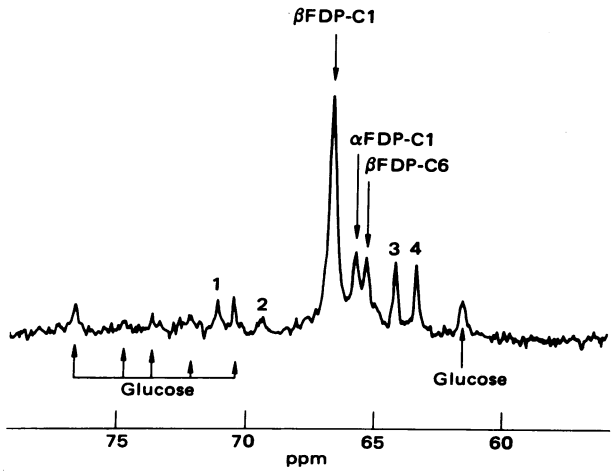

FIG. 5. The 55- to 85-ppm region of the 90.52-MHz ^{13}C NMR spectrum of glycolysing *E. coli* cells in the presence of [1-^{13}C]glucose. The spectrum was obtained from the same experiment as Fig. 3 by adding together six 1-min spectra that displayed constant Fru-1,6-P_2 (FDP) levels.

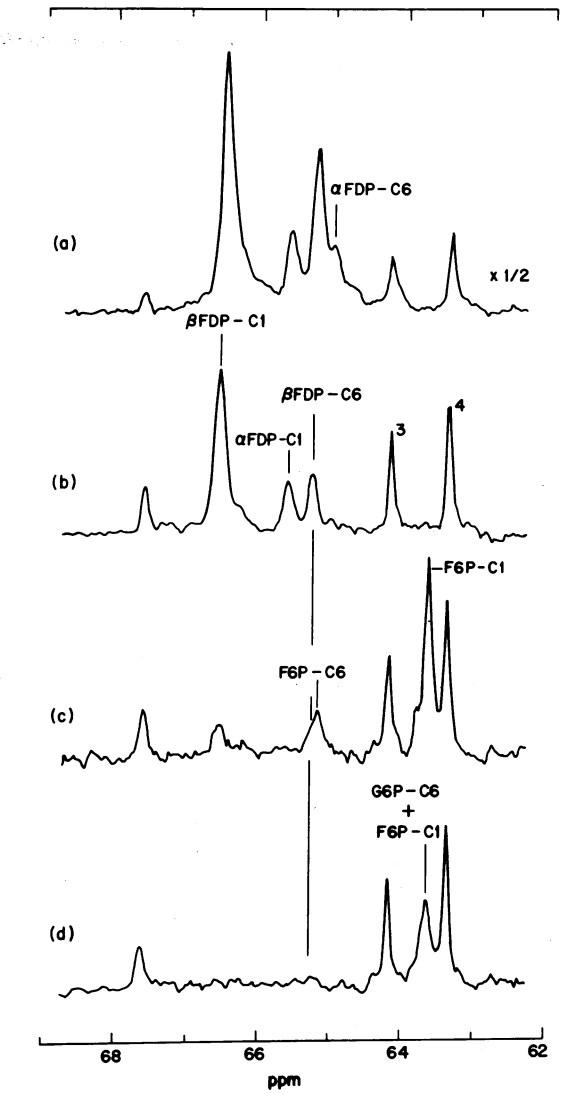

FIG. 6. An extract of anaerobic *E. coli* cells suspended under the experimental conditions of Fig. 3 was prepared by digestion with perchloric acid and subsequent neutralization with KOH (after the cellular debris was removed by centrifugation). The resultant solution was treated with Chelex 100 (Bio-Rad), lyophilized, and dissolved in distilled water (15% ^2H_2O). The 62- to 69-ppm region of the spectrum obtained from this extract (pH 7.5, 20°C) is shown in *b*. The sample was then divided into two portions. To one, Fru-1,6-P_2 (FDP) labeled approximately equally at the C-1 and C-6 positions was added (*a*). To the second sample, first 10 μl of hexosediphosphatase (Sigma, 50 units/ml) and $MgSO_4$ (final concentration, 5 mM in the extract) were added. After several hours of incubation at ambient temperature, spectrum *c* was obtained. To this solution, 5 μl of phosphohexose isomerase (Calbiochem, 4880 units/ml) was added. The resultant spectrum is given in *d*.

isomerase because the C-1 chemical shifts are very similar in Glc-6-*P* and glucose, and the extract spectrum contained very intense glucose peaks. However, both the disappearance of the Fru-6-*P* C-6 peak and the intensity loss at the combined position are as expected for phosphohexose isomerase catalyzed isomerization of Fru-6-*P*.

The observed synthesis of Fru-1,6-P_2 labeled at C-6 when [1-^{13}C]glucose is fed to the cells can occur as a consequence of scrambling of the label at the triosephosphate isomerase level coupled to back-synthesis of Fru-1,6-P_2 from the trioses by pathways through fructose bisphosphate aldolase or transaldolase.

The major resonances detectable after the onset of oxygenation (and which were absent in the anaerobic spectra) were

those of C-4, C-3, and C-2 of glutamate. Glutamate is assigned a central role in the synthesis of several amino acids. It itself is synthesized by direct amination of α-ketoglutarate, a tricarboxylic acid cycle intermediate. Because the ^{13}C–H dipole–dipole interaction is expected to be the dominant T_1 relaxation mechanism (22), glutamate C-2 and C-3 should have similar T_1 values whereas C-4 T_1 might be somewhat longer. Therefore, to a first approximation, the ratios of the peak intensities will reflect the actual distribution of the label between C-2 and C-3 of glutamate while underestimating the label in C-4. Note that the C-4 resonance (Glu4) is about twice as intense as the C-2 and C-3 peaks. [Fig. 4 gives peak heights; integrated intensities show C-2 and C-3 to be even closer (see Fig. 2).] Note also that, shortly after the acetate level starts dropping (Fig. 4), the glutamate C-4 intensity also begins to decrease, whereas the C-2 and C-3 intensities follow the succinate curve. It can be deduced from the known tricarboxylic acid cycle chemistry that a label entering the cycle as the methyl carbon of acetyl-CoA will, in the first turn of the cycle, be incorporated exclusively into glutamate C-4. If it proceeds to succinate, this label will be scrambled equally between C-2 and C-3 of succinate due to symmetry. In the second turn of the cycle, the label will then be incorporated into glutamate C-2 and C-3.

Alternatively, ^{13}C-enriched carbons can go directly into oxaloacetate from phospho*enol*pyruvate via phospho*enol*oxaloacetate (19); however, these will label only glutamate C-2 and C-3 in the first time through the cycle. Thus, the data indicate that, in our samples, the label is preferentially entering the tricarboxylic acid cycle as acetyl-CoA rather than as oxaloacetate (via phospho*enol*pyruvate and phospho*enol*oxaloacetate). This latter pathway, however, is responsible for succinate synthesis and accumulation under anaerobic conditions (19) (see Figs. 1 and 3). About 2 hr after the onset of oxygenation, as glutamate intensity decreases glutamine resonances appear. A possible explanation for this observation is that the unlabeled glutamine pool at this point is sufficiently decreased so that glutamine synthetase is activated.

Intensities of the resonances in the present spectra cannot be used to measure accurately the absolute concentrations of the detectable metabolites because our pulsing rate is faster than the expected spin-lattice relaxation rates. In addition, contributions of the nuclear Overhauser effect to the intensities may be different for each resonance. Despite these limitations, the time dependencies of the present resonances can still be used to obtain important kinetic information. From Fig. 3, it can be seen that the utilization rate of α-glucose increases in the first 1.5 min after glucose addition and remains approximately constant during the steady state between 1.5 and 8.5 min characterized by the time-independent Fru-1,6-P_2 concentration. The rate of β-glucose consumption, however, changes with time during the same period. The constant rate of α-glucose utilization during the glycolytic steady state suggests that this anomer has saturated the enzyme(s) responsible for its consumption. On the other hand, the inverse of the β-glucose utilization rate—calculated by first fitting the data to a polynomial and then taking its derivative—is linearly dependent on the inverse of its concentration during the 1.5- to 8.5-min "steady state"; this plot yields an apparent K_m of 7 mM. Thus, the steady-state points are consistent with the possible existence of two different anomer-specific sites involved in glucose translocation.

This model would require that the α-glucose-specific site have a small K_m (<1 mM); for β-glucose translocation, both K_m and V_{max} are larger. The data, including the points outside the 1.5- to 8.5-min range, can also be fitted satisfactorily to a model that assumes competition between α and β anomers for the same binding site. This model yields K_m values of ~4 and ~2.5 mM for the α and β anomers, respectively. The rapid utilization of glucose in *E. coli* is accomplished by the phospho*enol*pyruvate-dependent phosphotransferase system which affects the entry of glucose into the bacteria as Glc-6-*P* (23–25). Consequently, our results on glucose transport by *E. coli* are expected to apply to the properties of this system.

In summary, it has been shown that high-resolution ^{13}C NMR spectra contain considerable information about the distribution of the label in intermediates and end products that can be used in measuring metabolic rates and elucidating metabolic pathways *in vivo*.

J. A. den Hollander is the holder of a fellowship from the Netherlands Organization for the Advancement of Pure Research (ZWO).

1. Hoult, D. I., Busby, S. J. W., Gadian, D. G., Radda, G. K., Richards, R. E., & Seely, D. J. (1974) *Nature*, **252**, 285–287.
2. Navon, G., Ogawa, S., Shulman, R. G. & Yamane, T. (1977) *Proc. Natl. Acad. Sci. USA* **74**, 87–91.
3. Ugurbil, K., Rottenberg, H., Glynn, P. & Shulman, R. G. (1978) *Proc. Natl. Acad. Sci. USA* **75**, 2244–2248.
4. Moon, R. B. & Richards, J. H. (1973) *J. Biol. Chem.* **248**, 7276–7278.
5. Salhany, J. M., Yamane, T., Shulman, R. G. & Ogawa, S. (1975) *Proc. Natl. Acad. Sci. USA* **72**, 4966–4970.
6. Eakin, R. T., Morgan, L. O., Gregg, C. T. & Matwiyoff, N. A. (1972) *FEBS Lett.* **28**, 259–264.
7. Schaefer, J., Stejskal, E. O. & Beard, C. F. (1975) *Plant Physiol.* **55**, 1048–1053.
8. Matwiyoff, N. A. & Needham, T. E. (1972) *Biochem. Biophys. Res. Commun.* **49**, 1158–1164.
9. Tanabe, M. (1973) *Biosynthesis* **2**, 241.
10. Séquin, U., Scott, A. I. (1974) *Science* **186**, 101.
11. McInnes, A. G., Wright, J. L. C. (1975) *Acc. Chem. Res.* **9**, 313.
12. McInnes, A. G., Walter, J. A., Wright, J. L. C. & Vining, L. C. (1976) in *Topics in Carbon-13 NMR Spectroscopy*, ed. Levy, G. C. (Wiley Interscience, New York) Vol. 2, p. 123.
13. Smith, I. C. P., Jennings, H. J. & Des Lauriers, R. (1975) *Acc. Chem. Res.* **8**, 306–313.
14. Eakin, R. T., Morgan, L. O. & Matwiyoff, N. A. (1975) *Biochemistry* **152**, 529–535.
15. Kainosho, M., Ajisaka, K. & Nakazawa, H. (1977) *FEBS Lett.* **80**, 385–389.
16. Gorin, P. A. J. & Mazurek, M. (1975) *Can. J. Chem.* **53**, 1212–1223.
17. Koerner, T. A. W., Cary, L. W., Bhacca, N. S. & Younathan, E. S. (1973) *Biochem. Biophys. Res. Commun.* **51**, 543–550.
18. Horsley, W., Sternlicht, H. & Cohen, J. S. (1970) *J. Am. Chem. Soc.* **92**, 680.
19. Doelle, H. W. (1975) *Bacterial Metabolism*, (Academic, New York).
20. Lehninger, A. L. (1970) *Biochemistry*, (Worth, New York).
21. Benkovic, S. J., Engle, J. L. & Mildvan, A. S. (1972) *Biochem. Biophys. Res. Commun.* **47**, 852–858.
22. Kuthman, K. F., Grand, D. M. & Harris, R. K. (1970) *J. Chem. Phys.* **52**, 3439–3448.
23. Kundig, W., Ghosh, S. & Roseman, S. (1964) *Proc. Natl. Acad. Sci. USA* **52**, 1067–1074.
24. Roseman, S. (1975) *Ciba Found. Symp.* **31**, 225–241.
25. Kornberg, H. L. (1975) in *Biochemical Society Transactions 558th Edinburgh Meeting*, Vol. 3, p. 835–837.